ornl

OAK RIDGE NATIONAL LABORATORY

UNION CARBIDE

ORNL/TM--7927

DE82 004652

MASTER

Calculation of Neutron and Gamma-Ray Energy Spectra for Fusion Reactor Shield Design: Comparison with Experiment II

R. T Santoro
R G. Alsmiller, Jr.
J M. Barnes
G T Chapman

OPERATED BY
UNION CARBIDE CORPORATION
FOR THE UNITED STATES
DEPARTMENT OF ENERGY

ORNL/TM-7927
Dist. Category UC-20d

Contract No. W-7405-eng-26

Engineering Physics Division

CALCULATION OF NEUTRON AND GAMMA-RAY ENERGY SPECTRA FOR FUSION REACTOR SHIELD DESIGN: COMPARISON WITH EXPERIMENT II*

R. T. Santoro
R. G. Alsmiller, Jr.
J. M. Barnes+
G. T. Chapman

Date Published - November 1981

*Submitted for
Journal publication

+UCC-ND Computer Sciences Division

This Work Sponsored by
Office of Fusion Energy
U.S. Department of Energy

OAK RIDGE NATIONAL LABORATORY
Oak Ridge, Tennessee 37830
operated by
UNION CARBIDE CORPORATION
for the
DEPARTMENT OF ENERGY

TABLE OF CONTENTS

I. INTRODUCTION

A series of integral experiments are being performed at the Oak Ridge National Laboratory to provide experimental verification of the nuclear data and radiation transport methods that are being used in the nuclear design calculations for fusion reactors.[1,2] In this paper, measured and calculated neutron and gamma-ray energy spectra resulting from the transport of ∿14 MeV neutrons through a 0.30-m-thick lithium hydride (LiH) and through 0.05 m of lead (Pb) followed by 0.30 m of LiH are compared as a function of detector location. Also reported are comparisons of the measured and calculated neutron energy spectra as a function of detector location behind a 0.80-m-thick assembly comprised of stainless steel type-304 (SS-304) and borated polyethylene (BP). The spatial dependence of the gamma-ray energy deposition rate in the SS-304-BP assembly measured using calcium-flouride (manganese activated) thermoluminescent dosimeters (TLDs) is compared with calculated data obtained using radiation transport methods.

The LiH and Pb-LiH assemblies simulate blanket compositions and configurations and the 0.80-m-thick SS-304-BP assembly represents a thick shield configuration. In a previous paper,[1] measured and calculated neutron and gamma-ray spectra were compared for SS-304-BP slab configurations up to 0.56-m-thick and the work reported here for the SS-304-BP assembly is a continuation of that study and is of interest in determining the effectiveness of the calculational methods in determining transport of ∿14 MeV neutrons in a thick shield.

The experimental and calculational procedures are described in Section II and the measured and calculated data are presented and discussed in Section III.

II. EXPERIMENTAL AND CALCULATIONAL PROCEDURES

The experimental facility for performing the integral measurements is shown in an artist's rendition in Fig. 1. The important components include an electrostatic generator, a tritium-target source can assembly, a concrete test slab support structure, the neutron-gamma-ray detection system, and a thermal neutron shield. The details of the experimental and calculational procedures used to obtain the neutron and gamma-ray spectra have been described in detail in Refs. 1-3, so only a brief discussion of these procedures is given here.

A. Experimental Procedures

The experiments are carried out using ∿14 MeV neutrons having a source strength of $\sim 10^8$ n/s produced in the interactions of 250 keV deuterons with 4 mg/cm^2 of tritium saturated in a titanium target. The neutrons are produced via the

$$D + T \rightarrow n + {}^4He + 17.6\ MeV \qquad (1)$$

reaction. The target is enclosed in a cylindrical, re-entrant iron can which has the functions of shaping the neutron spectrum incident on the test slabs and of reflecting neutrons emitted in the backward direction towards the test slabs. The iron source can was carefully designed to modify the D-T neutron source distribution emanating from the can to make it characteristic of that incident on the first wall of a fusion reactor.[3] The target, iron can, and the test slabs are supported by the concrete test slab support structure. The concrete forming the structure is sufficiently thick to act as an environmental shield and minimize the radiation background level in the vicinity of the detector.

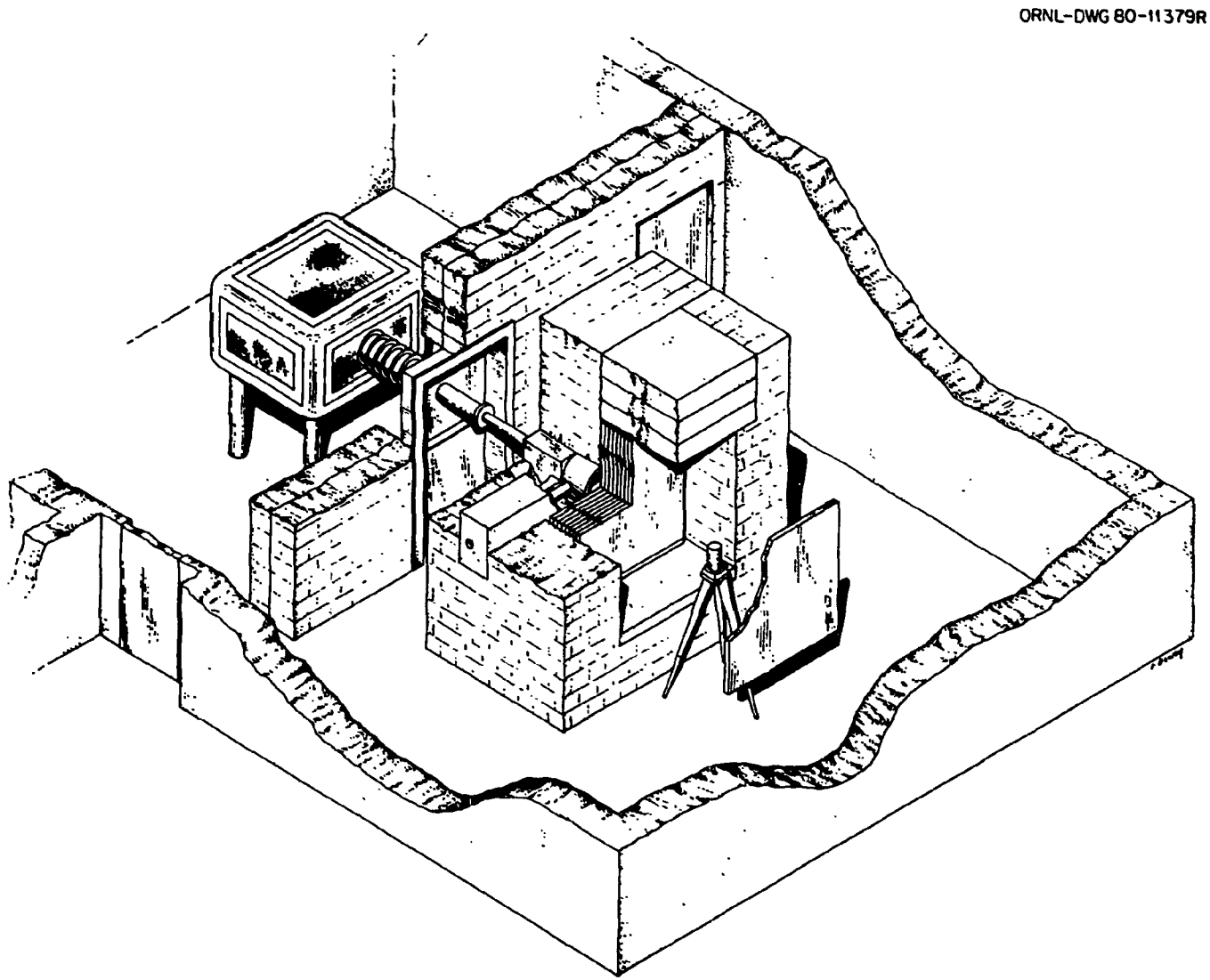

Fig. 1. Artist's rendition of the experimental facility.

The experiment test slabs (1.52x1.52 m^2) are inserted in the cavity in the concrete structure. (In some cases, however, the test slabs have a cross-sectional area that is larger than the cross-sectional area of the cavity. These slabs are mounted outside of the cavity against the face of the concrete structure.)

The neutron and gamma-ray energy spectra are measured at various positions relative to the deuteron-tritium target axis and as a function of the test slab composition and thickness using a 0.047 m diameter by 0.047 m high NE-213 liquid scintillator mounted on a RCA 8850 photomultiplier tube. Neutron and gamma ray events in the detector are separated using pulse-shape discrimination methods and are stored in separate memory locations in a ND-812 pulse-height analyzer computer. The neutron and gamma ray pulse-height data were normalized to the absolute neutron yield from the target which was determined using associated particle counting methods. The uncertainty in the neutron source strength has been determined to be ± 3%.[4]

The pulse-height data were obtained for neutrons with energies above 850 keV and for gamma rays with energies above 750 keV. The neutron and gamma ray pulse-height data were unfolded using the FERD[5] computer program to produce the energy spectra. The neutron response matrix used to unfold the spectra was obtained from measurements using the pulsed neutron beam from the Oak Ridge Linear Accelerator[1] and the gamma ray response matrix was generated using gamma ray sources of known energies. The total response of the NE-213 detector is known to within 5%. Gain calibrations were determined to be reproducible to within 2%.[4] The energy resolution of the detector was shown to vary as

$$R_N = [300 + 800/E_N]^{1/2} \qquad (2)$$

for neutrons of energy E_N and as

$$R_\gamma = [170 + 288/E_\gamma]^{1/2}$$

for gamma rays of energy E_γ. R_N and R_γ are the full width of half-maximum (in percent) of the detector response to neutrons or gamma rays.

B. Calculational Procedures

The calculated neutron and gamma ray energy spectra were obtained using two-dimensional radiation transport methods. The experimental configuration was represented in r-z geometry with cylindrical symmetry about the deuteron beam axis. The calculational models used to estimate the transport of ∿14 MeV neutrons through the LiH and Pb plus LiH slabs and through the SS-304-BP assembly are shown in Figs. 2 and 3, respectively. The geometry shown in Fig. 2 is represented using 42 radial and 92 axial mesh intervals. The cross-sectional dimensions of the LiH and Pb slabs were larger than those of the cavity in the concrete structure so they were, by necessity, positioned on the face of the structure as shown in Fig. 2. The geometry in Fig. 3 was represented using 42 radial and 91 axial mesh intervals. In this measurement, the SS-304 and BP were positioned inside of the cavity. Also shown in the figure are the locations of the TLDs that were used to measure the gamma-ray energy deposition rates in the test slab assembly.

The sequence of radiation transport calculations used to obtain the neutron and gamma ray energy spectra and the photon energy deposition rates is shown in Fig. 4 and is very similar to that described in Ref. 1. The sequence is initiated using the GRTUNCL code[6] to obtain the uncollided neutron flux and first collision source distributions at all spatial mesh

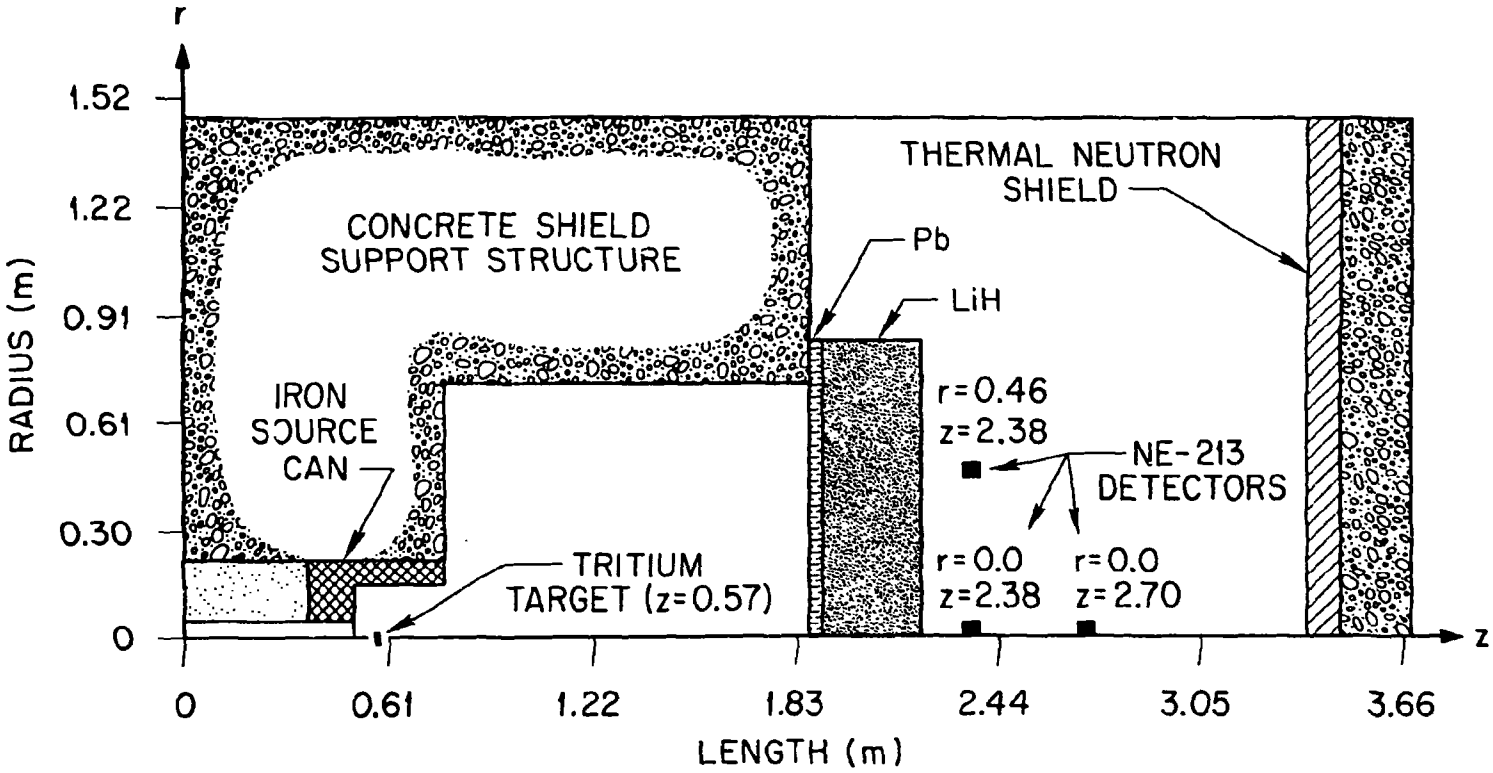

Fig. 2. Two-dimensional calculational model of the experimental configuration for LiH and Pb+LiH slab measurements.

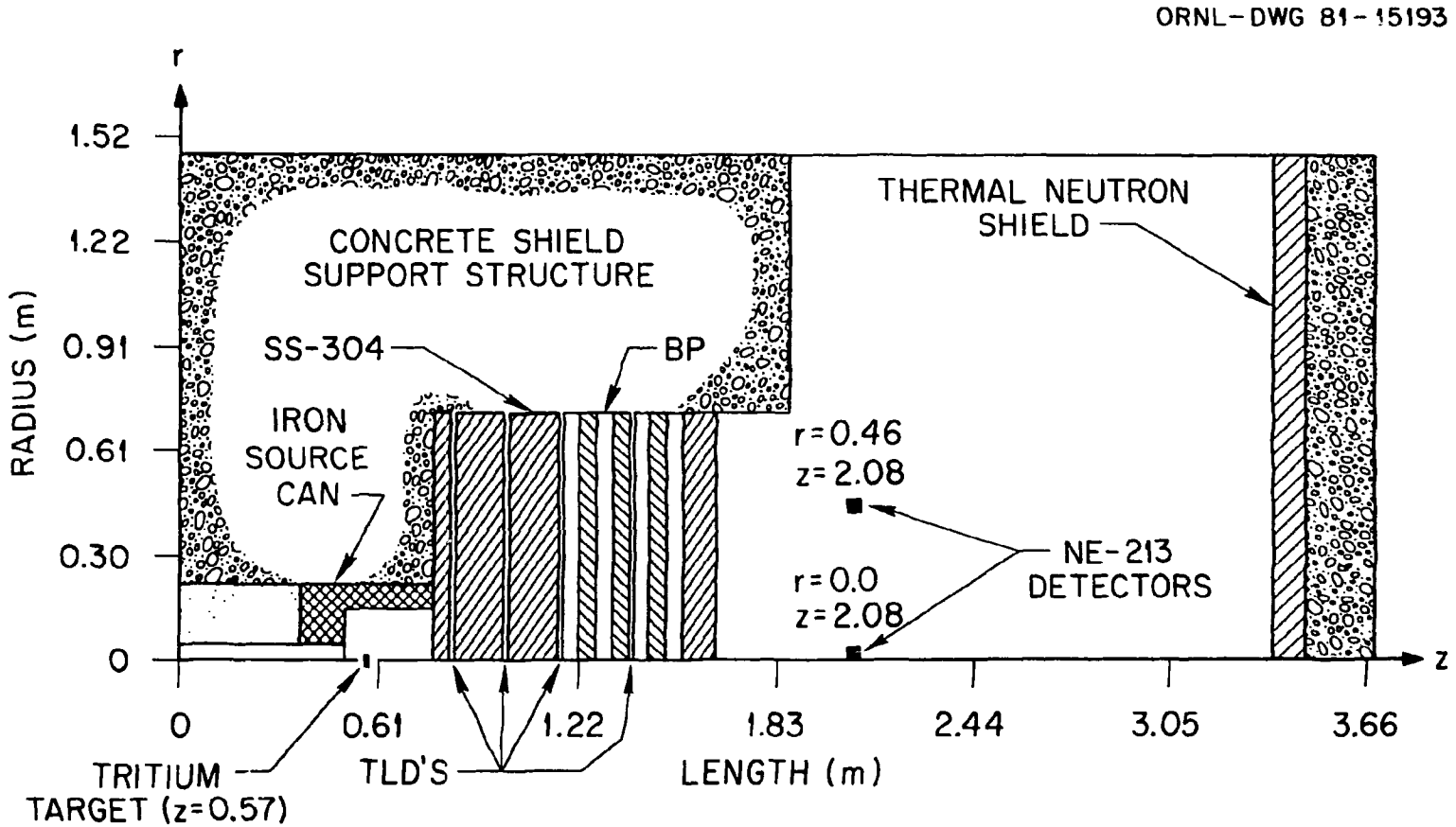

Fig. 3. Two-dimensional calculational model of the experimental configuration for the 0.80-m-thick SS-304-BP measurements.

intervals in the calculational geometry. The source term for the GRTUNCL code was obtained by calculating the angle-energy dependence of the neutrons emitted from the reactions of 250 keV deuterons in the tritium target and weighting the neutron emission probabilities by appropriate solid angle factors to account for the anisotropy of the neutron source in the GRTUNCL code. The calculational procedure used to obtain the angle-energy dependence of the emitted neutrons is described in detail in Ref. 3. The first collision source data from GRTUNCL is input to the two-dimensional discrete ordinates code DOT.[7] This code calculates the collided flux distributions using the first collision data as a spatially distributed source. These calculations were completed using an S_{12} angular quadrature. A final scattering source tape is generated in DOT and is employed to carry out a last-flight transport calculation using the FALSTF code[8] to obtain the neutron and gamma-ray energy-dependent flux at each detector center location. The output from FALSTF is combined with the uncollided flux data from GRTUNCL to yield the total flux at each detector location. These total fluxes are processed to obtain the neutron and gamma-ray energy spectra by smoothing the flux per unit energy in each multigroup energy interval with an energy-dependent Gaussian response function having a width determined by Eq. (2) for neutrons, and Eq. (3) for gamma rays. Performing the calculations in the sequence shown in Fig. 4 assures that ray effects from the D-T neutron source are eliminated, as well as those from intense last collision sources from neutron reactions with experimental components.

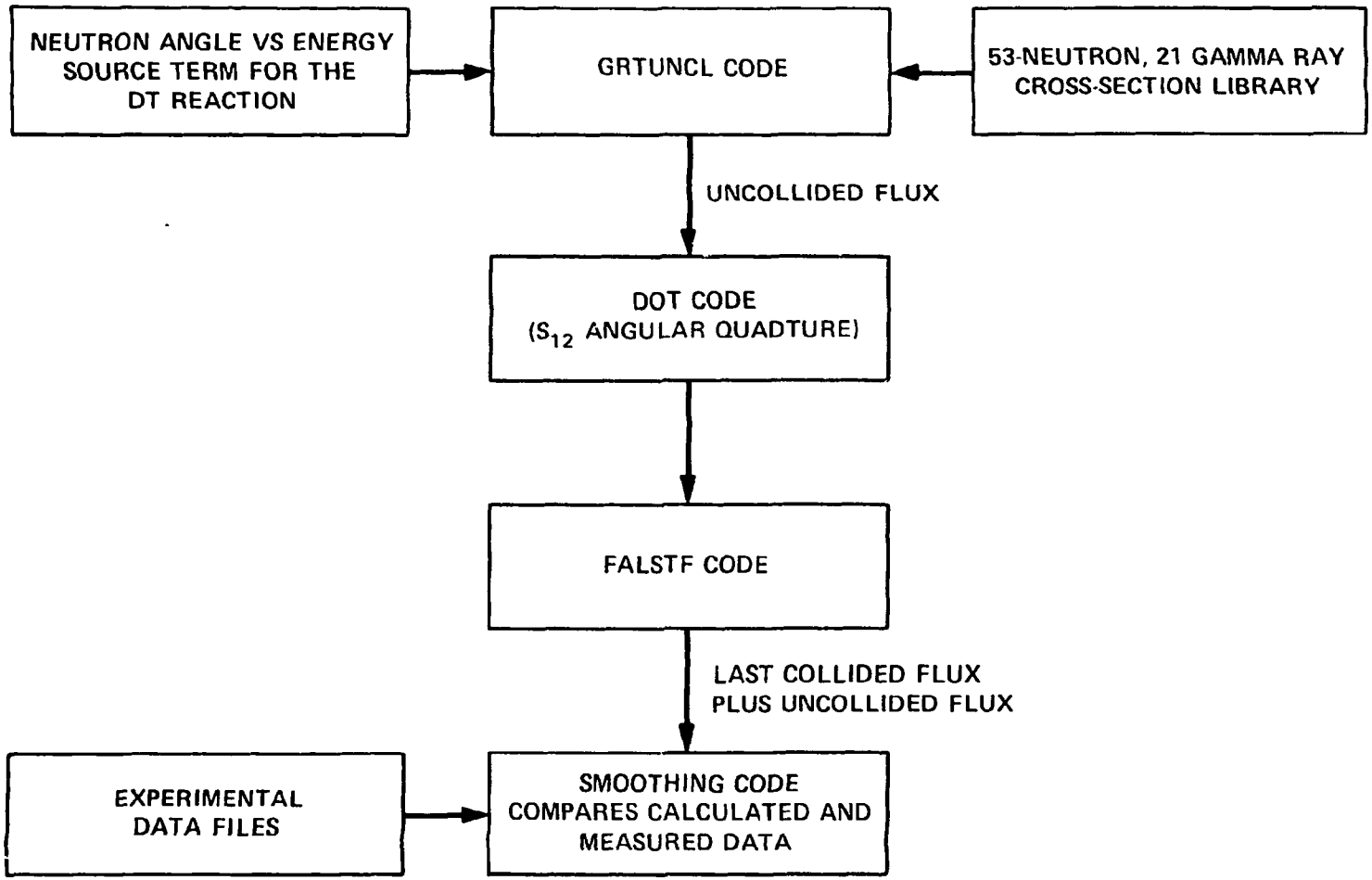

Fig. 4. Sequence of calculations to obtain neutron and gamma-ray energy spectra.

The radiation transport calculations incorporated a 53-neutron, 21-gamma-ray energy group library obtained by collapsing the 171-neutron, 36-gamma-ray VITAMIN C data library (ENDF/B-IV).[9] The VITAMIN C library was created as a general purpose cross section data set for the analysis of fusion neutronics problems. The fine-group library was collapsed using the ANISN[10] code by representing the experimental components in spherical geometry and using the neutron emission probabilities as the weighting functions. The energy boundaries of the 53-neutron library, were based in part on those used in the DLC-47 library,[11] but expanded at high energies so that the D-T neutron source could be more accurately represented in the transport calculations. The angular dependence of the cross sections for all nuclei was approximated using a P_3 Legendre expansion. The composition of the materials used in the calculations is given in Table I.

III. DISCUSSION OF RESULTS

A. LiH and Pb+LiH Assemblies

The measured and calculated differential neutron energy spectra behind the LiH and Pb plus LiH slabs as a function of detector location are compared in Figs. 5 and 6, respectively. In Fig. 5, the spectra are compared for the cases when the detector is on (r = 0.0) and off (r = 0.46 m) the axis of symmetry at z = 2.38 m and in Fig. 6 the spectra are compared when the detector is on the axis at z = 2.70 m. The source-to-detector distance along the z-axis is obtained by subtracting 0.57 m from the given z values. The solid curves are the measured spectra and the points are the calculated data. The measured data were obtained by unfolding the pulse-height data and for some of the spectra in Figs. 5 and 6, as well

Table I. Composition of Materials[a]

Element	Composition (Atom/cm·barn)						
	Lithium Hydride	Lead	SS-304	BP[b]	Concrete	Air	Iron
H	6.21-2			7.13-2	7.86-3		
Li-6	4.61-3						
Li-7	5.75-2						
B-10				4.87-4			
B-11				1.97-3			
C				3.41-2			
N						3.64-5	
O				3.54-3	4.39-2	9.74-6	
Na					1.05-3		
Mg					1.40-4		
Al					2.39-3		
Si					1.58-2		
K					6.90-4		
Ca					2.92-3		
Cr			1.77-2				
Mn			1.77-3				
Fe			6.02-2		3.10-4		8.48-2
Ni			7.83-3				
Pb		3.34-2					

[a]Lead, air, and iron compositions are theoretical. All others are within ±5% of compositions determined from chemical assays. No impurity concentrations are included in SS-304 composition.

[b]BP = Borated Polyethylene.

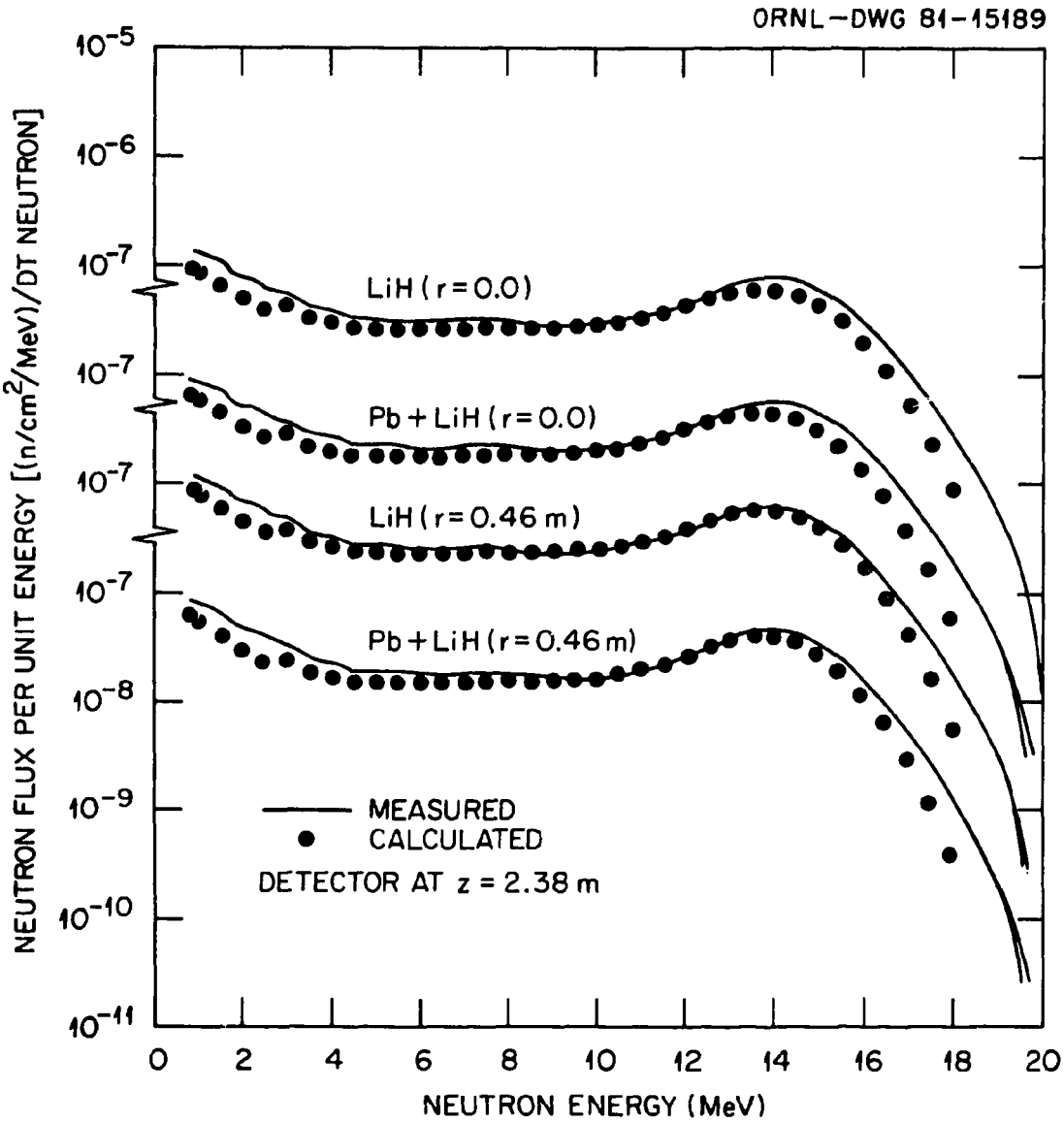

Fig. 5. Neutron flux per unit energy vs. neutron energy for the LiH and Pb plus LiH slab assemblies for the detector at z = 2.38 m; r = 0.0 and r = 0.46 m. (Note breaks in the ordinate)

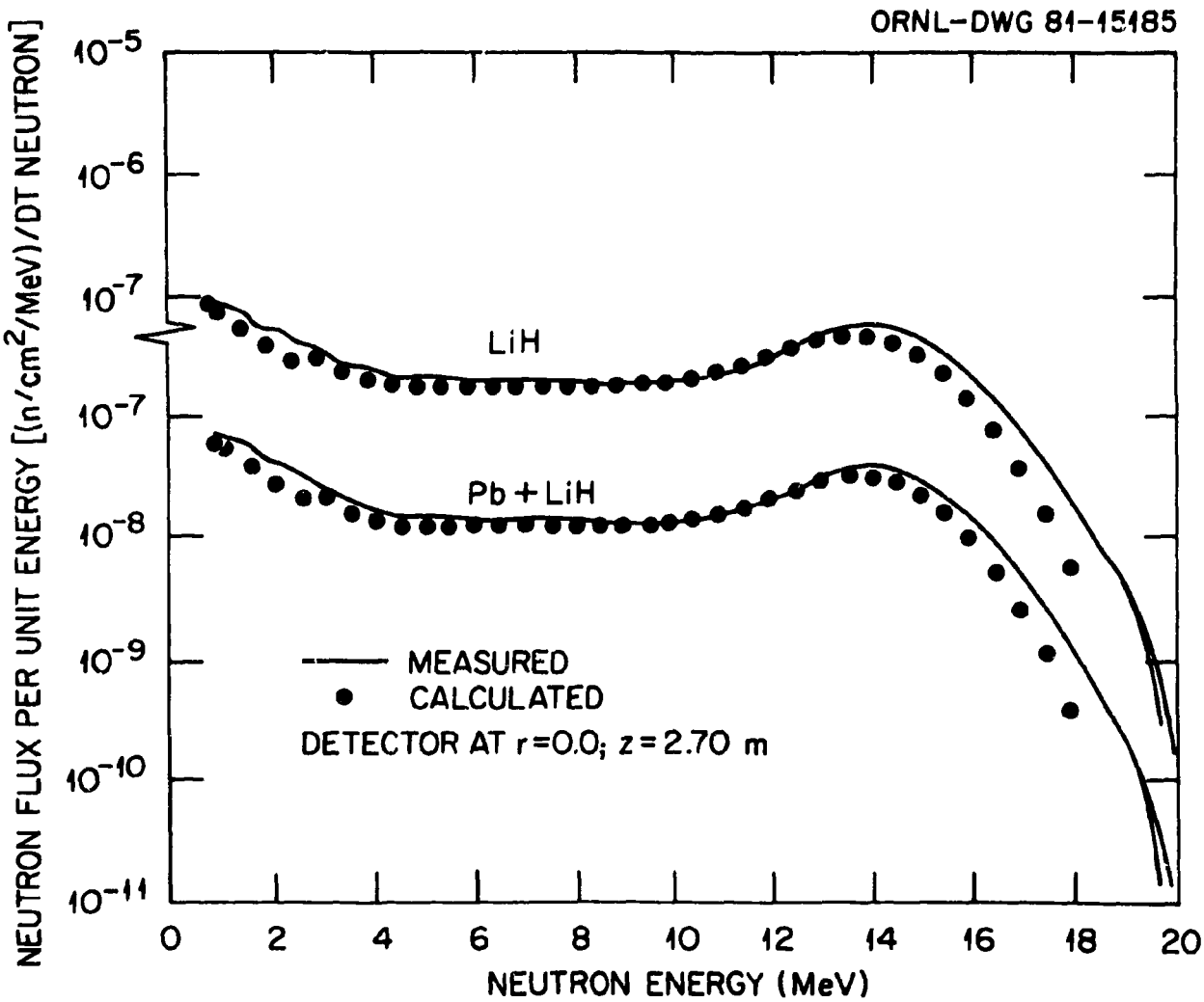

Fig. 6. Neutron flux per unit energy vs. neutron energy for the LiH and Pb plus LiH slab assemblies for the detector at z = 2.70 m, r = 0.0 m. (Note break in the ordinate)

as those given below, two curves are shown. The two curves indicate a 68% confidence interval in the unfolded spectra. The calculated data were obtained by smoothing the flux per unit energy in each multigroup energy interval with an energy-dependent Gaussian response function having a width defined by Eq. (2). It is not kinematically possible for 250 keV deuterons to produce neutrons with energies above 15.1 MeV. The indication of more energetic neutrons in the spectra is a manifestation of the Gaussian response of the neutron detector used to smooth the data.

The calculated and measured neutron energy spectra are in reasonably good agreement for both the LiH and Pb plus LiH slab assemblies at all detector locations. At neutron energies below ∿6 MeV, the calculated data are lower than the measured data with differences ranging from ∿10% to nearly a factor of two depending on the neutron energy. This systematic behavior prevails at all detector locations and whether or not the lead is present in the assembly. When the lead is included, the principal effect is a reduction in the magnitude of the neutron flux per unit energy by nearly a factor of two at all neutron energies. The shapes of the calculated and measured spectra do, however, remain the same.

The integrated neutron energy spectra, obtained by integrating the spectra in Figs. 5 and 6, are shown in Figs. 7 and 8, respectively. The measured and calculated data are in good agreement for both the LiH and Pb plus LiH slab configurations and at all detector locations. The calculated integral data agree with the measured integrated spectra within ∿5% to ∿20% except at neutron energies above ∿15 MeV where the difference is due to the Gaussian smoothing of the data rather than cross section or neutron transport effects.

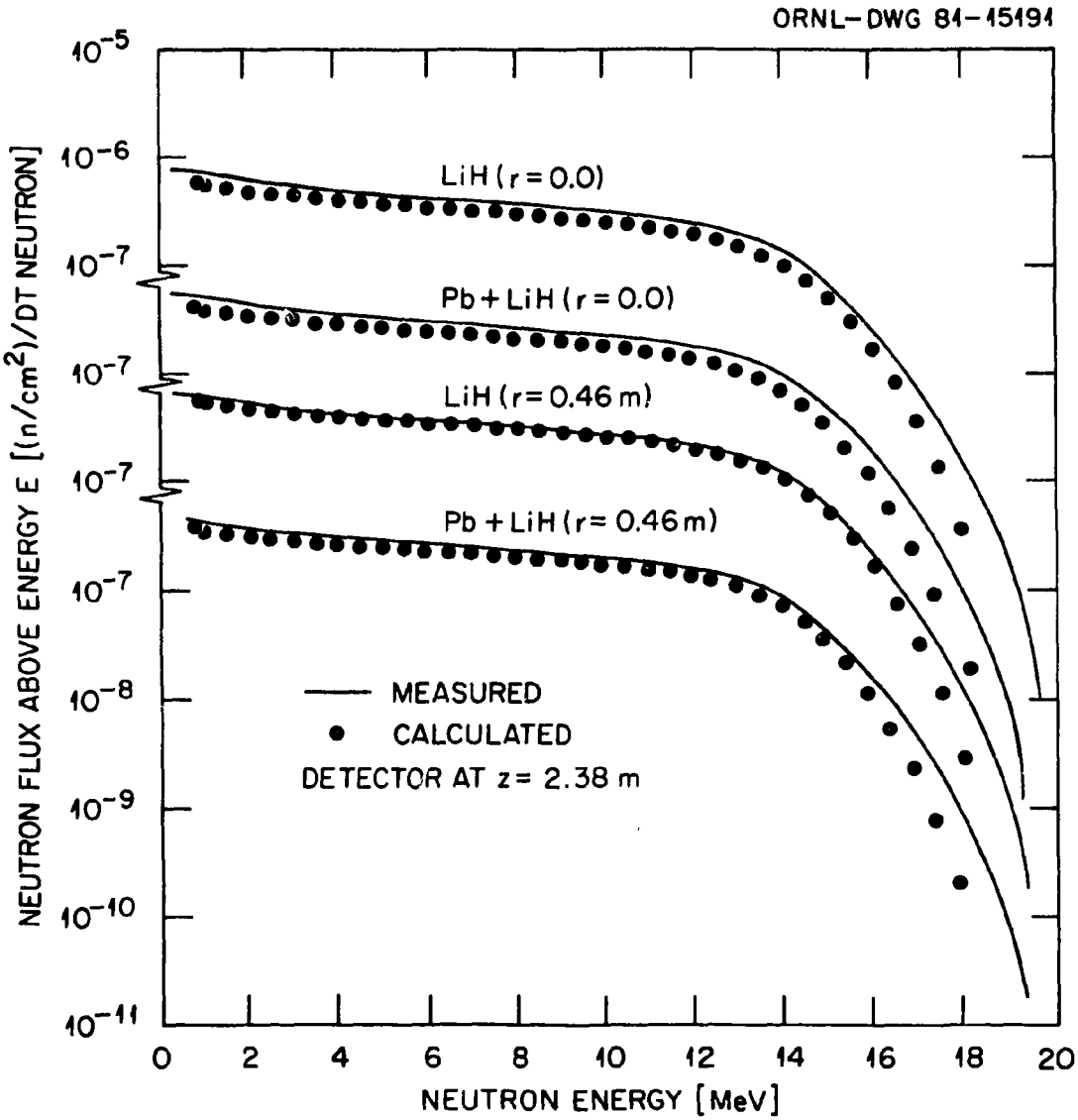

Fig. 7. Neutron flux above energy E vs. neutron energy for the LiH and Pb plus LiH slab assemblies for the detector at z = 2.38 m, r = 0.0 and r = 0.46 m. (Note breaks in the ordinate)

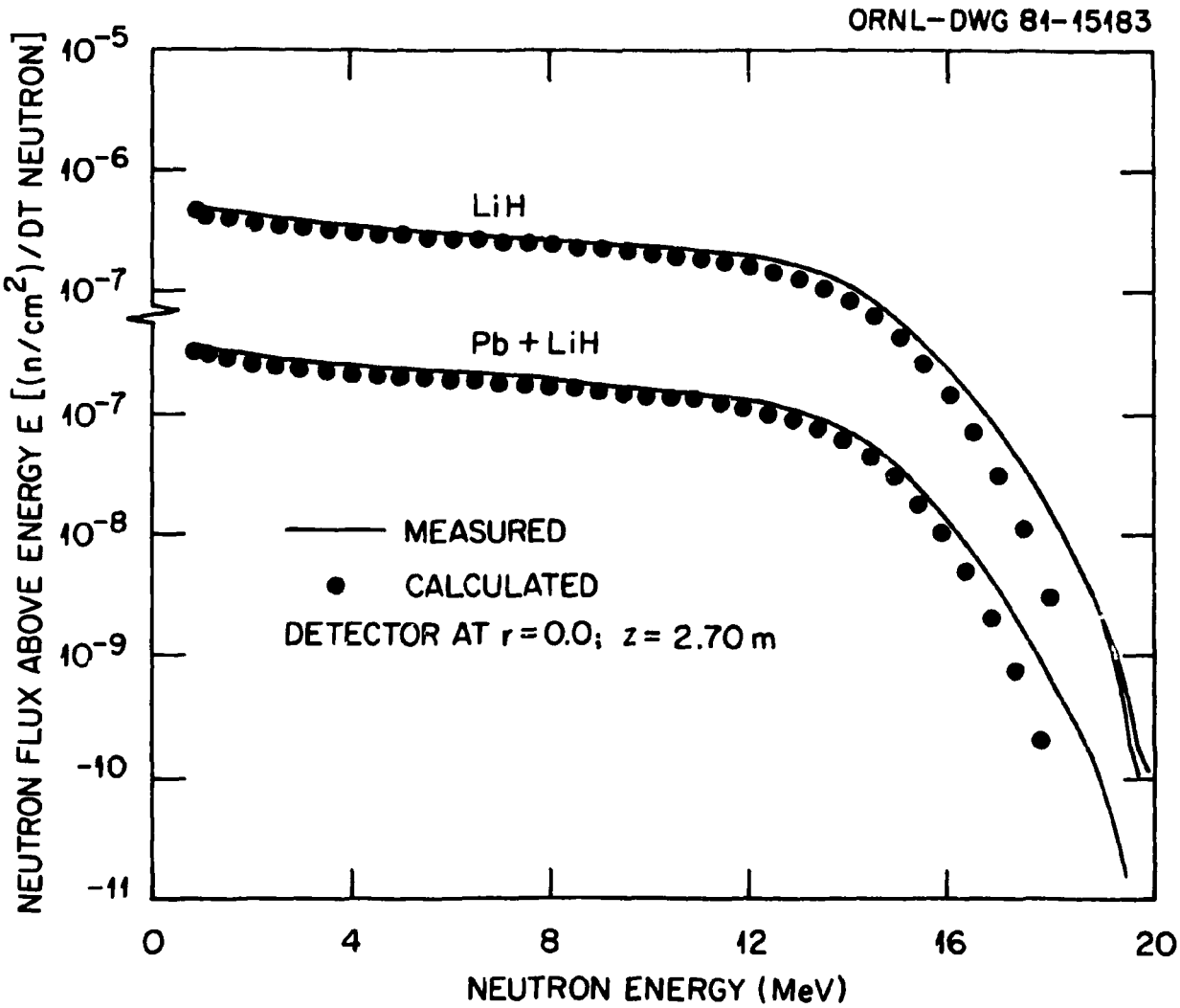

Fig. 8. Neutron flux above energy E vs. neutron energy for the LiH and Pb plus LiH slab assemblies for the detector at z = 2.70 m, r = 0.0 m. (Note break in the ordinate)

The measured and calculated differential and integral gamma-ray energy spectra as a function of detector location behind the LiH and Pb plus LiH slabs are compared in Figs. 9-12.

The calculated and measured differential and integral energy spectra behind the LiH slabs are in excellent agreement for gamma ray energies up to ∿10 MeV. The calculation reproduces the spectra in magnitude, and within the limits of the broad energy group structure, accounts for the structure in the measured spectra as well. For the Pb plus LiH slabs, however, the agreement among the calculated and measured data is less favorable. The differential spectra are in good agreement up to ∿5 MeV, but at higher energies the calculated data are lower than the measured data by about a factor of three. Thermal neutron capture in lead yields gamma rays of 6.5 MeV (5%) and 7.2 MeV (95%). These lines appear in the measured spectra but are not accounted for in the calculated data. The failure of the calculation to reproduce these gamma rays can be attributed to either the thermal neutron capture cross section or the thermal neutron transport in the calculational model. The shape in the spectra for the LiH case is well produced up to 10 MeV. The 7 MeV gamma ray from neutron capture in Li as well as the 2.25 MeV photon from capture in hydrogen are accounted for in both assemblies which suggests that the thermal neutron flux is being calculated correctly in LiH and that the capture cross section or photon multiplicity may not be correct in the ENDF/B-IV data files for Pb.

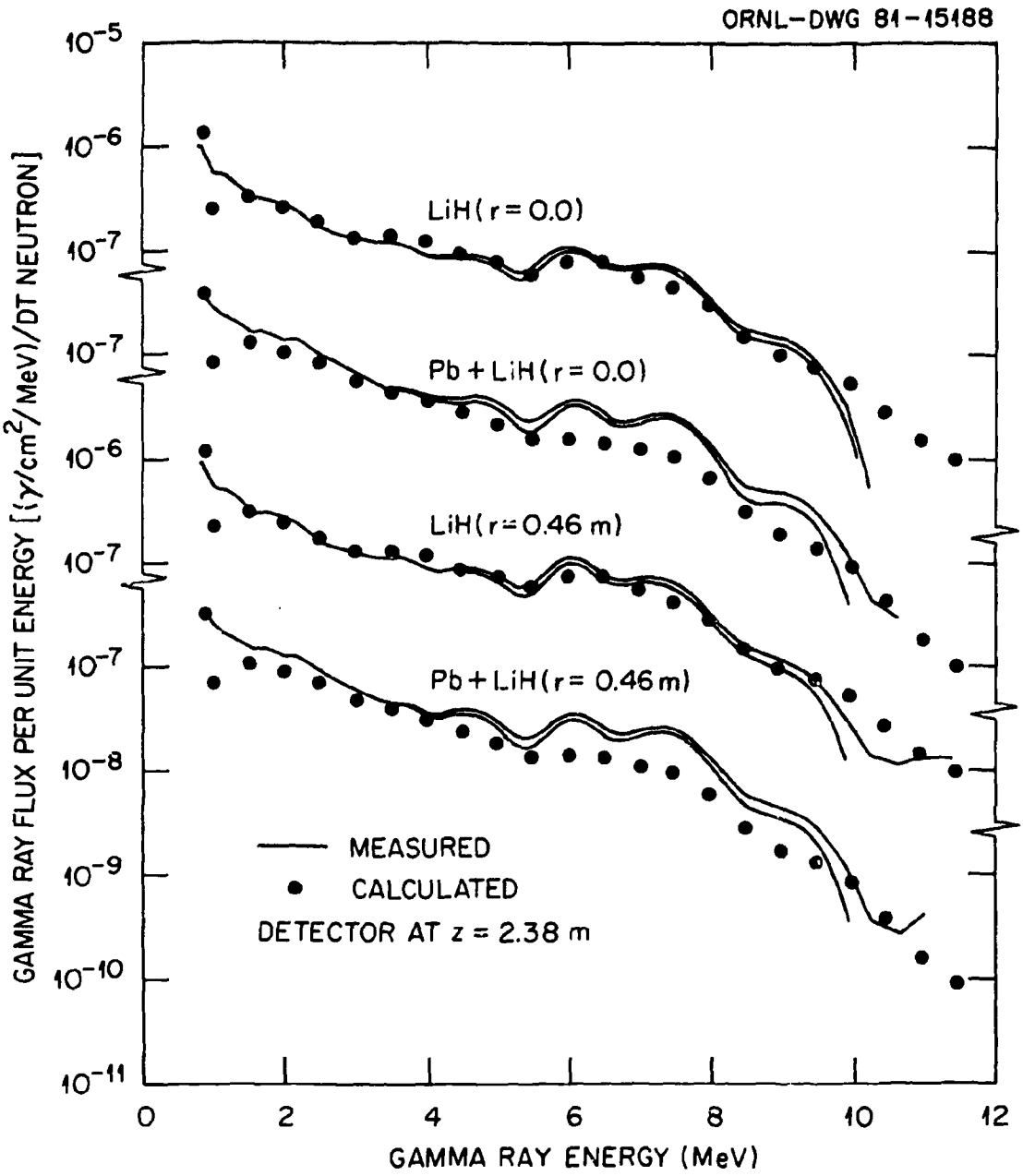

Fig. 9. Gamma-ray flux per unit energy vs. gamma-ray energy for the LiH and Pb plus LiH slab assemblies for the detector at z = 2.38 m, r = 0.0 and r = 0.46 m. (Note breaks in the ordinate)

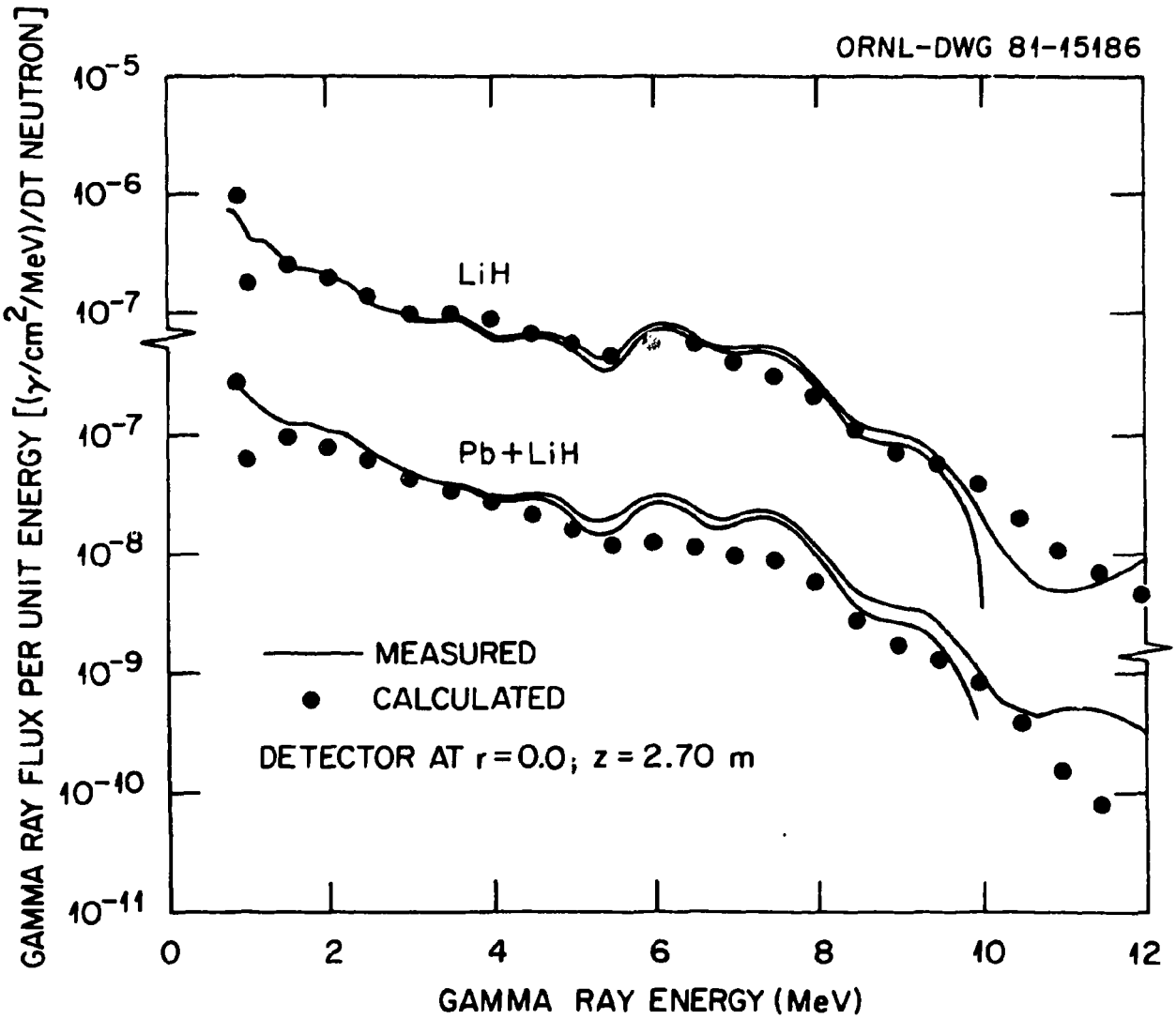

Fig. 10. Gamma-ray flux per unit energy vs. gamma-ray energy for the LiH and Pb plus LiH slab assemblies for the detector at z = 2.70 m, r = 0.0 m. (Note break in the ordinate)

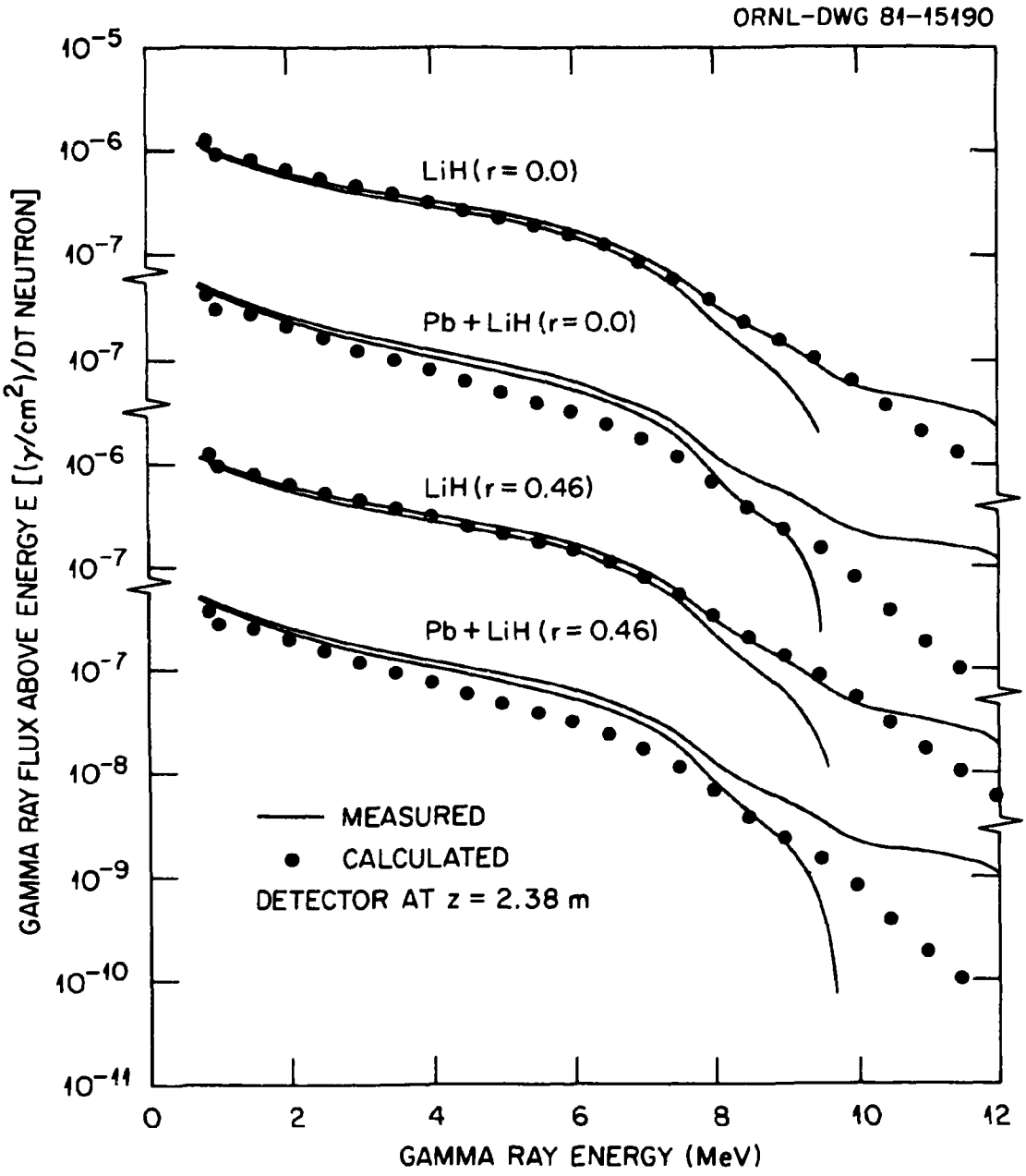

Fig. 11. Gamma-ray flux above energy E vs. gamma-ray energy for the LiH and Pb plus LiH slab assemblies for the detector at z = 2.38 m. r = 0.0 and r = 0.46 m. (Note breaks in the ordinate)

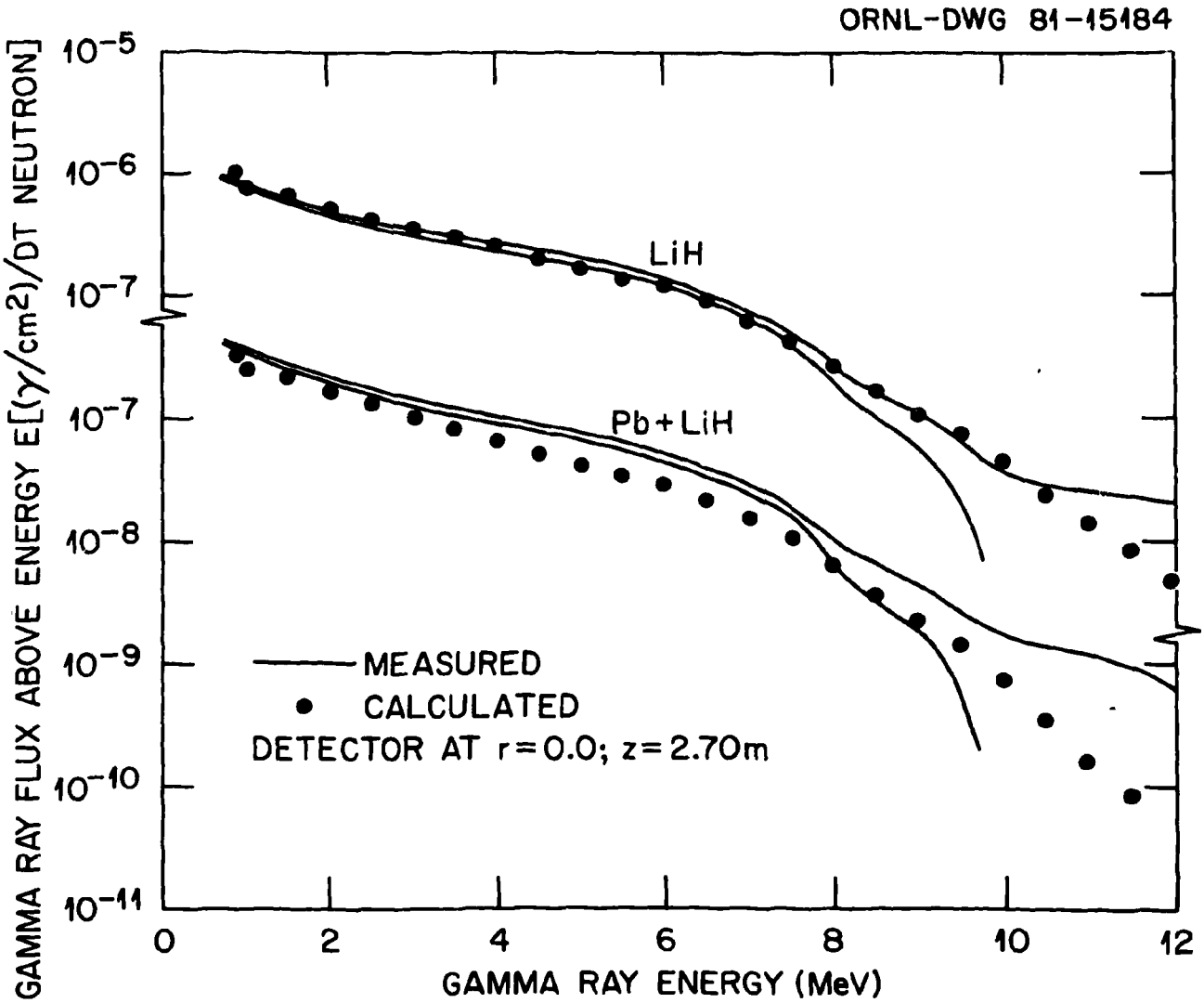

Fig. 12. Gamma-ray flux above energy E vs. gamma-ray energy for the LiH and Pb plus LiH slab assemblies for the detector at z = 2.70 m and r = 0.0 m. (Note breaks in the ordinate)

B. SS-304-BP Shield Assembly

The calculated and measured differential neutron energy spectra at the two detector locations shown in Fig. 3 for the 0.80-m-thick SS-304-BP slab assembly are compared in Fig. 13. The composition and dimensions of the assembly are given in Table II.

The calculated and measured neutron energy spectra are in excellent agreement above ∿5 MeV at both detector locations. However, at neutron energies below ∿5 MeV, the calculated neutron flux per unit energy is lower than the measured data by as much as a factor of three depending on the detector location and neutron energy. Note that the measured data are indicated by a dashed line below 5 MeV. This is done to indicate that the data are very uncertain at these energies. Since the SS-304-BP slab assembly is very thick, the low energy neutron spectrum was not well defined since the flux leaking from the assembly is comparable with the neutron flux leaking through the concrete support structure.

The comparisons of measured and calculated gamma-ray spectra also revealed a very similar and more serious behavior and, for that reason, are not shown here. Since these measurements were made, the experimental facility has been reconstructed at a facility where the background levels from radiation leaking through the concrete are anticipated to be much lower than in the facility used for these studies and the experiment will be repeated to resolve the anomalies in the measured low energy neutron and gamma ray data.

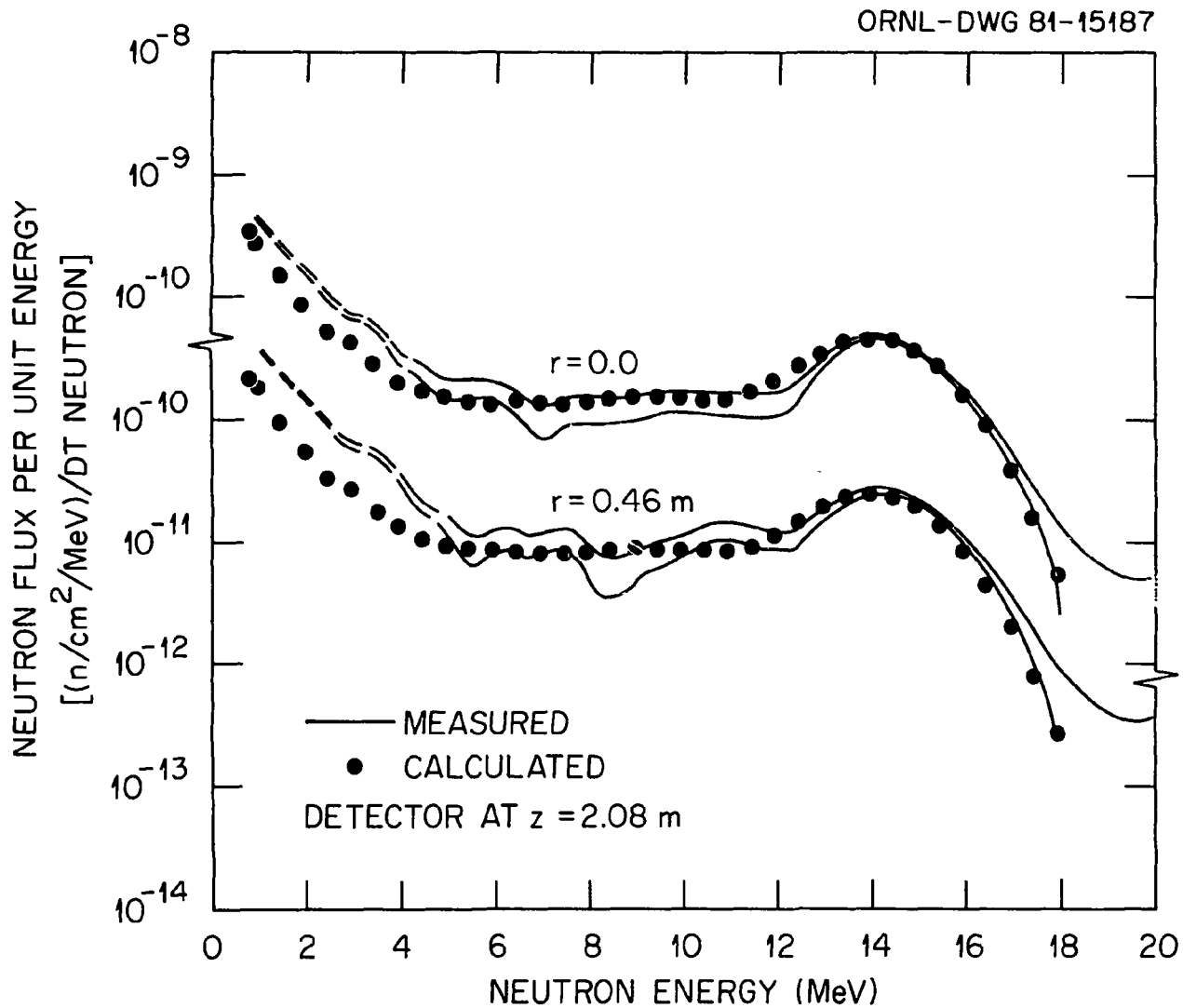

Fig. 13. Neutron flux per unit energy vs. neutron energy for the 0.80-m-thick SS-304-BP assembly for the detector at z = 2.08 m, r = 0.0 and r = 0.46 m. (Note break in the ordinate)

Table II. Theoretical Composition and Thickness of SS-304-BP Slab Assembly[a]

Material	Thickness	
	cm	g/cm^2
SS-304	5.08	39.97
SS-304	15.24[b]	119.93
SS-304	15.24[b]	119.93
BP	5.08	5.77
SS-304	5.08	39.97
BP	5.08	4.77
SS-304	5.08	39.97
BP	5.08	4.77
SS-304	5.08	39.97
BP	5.08	4.77
SS-304	5.08	39.97
SS-304	5.08	39.97
	81.3	498.72

[a]The actual thickness of the slabs does not vary by more than ±2%.

[b]Three 5.08-cm-thick slabs combined to form a single 15.24-cm-thick slab.

The measured and calculated integral neutron energy spectra are compared in Fig. 14. The data are in excellent agreement over the neutron range from 3 to 15 MeV and agree to within better than a factor of two between 850 keV and 3 MeV.

The calculated and measured gamma ray energy deposition rates (MeV/g/min) as a function of the SS-304-BP slab thickness are compared in Fig. 15. The measured data were obtained using calcium-flouride (manganese activated) thermoluminescent detectors (TLDs) located in gaps between the various slabs (see Fig. 3). The calculated data were obtained by convoluting the gamma ray flux obtained from the radiation transport calculations with the TLD response functions of Maerker.[12]

The measured and calculated dose equivalent rates are in reasonably good agreement at all detector locations. The calculated data are lower than the measured data but are, in all cases, within a factor of two of the measured data. The uncertainties in the measured data are estimated to be ±5%.

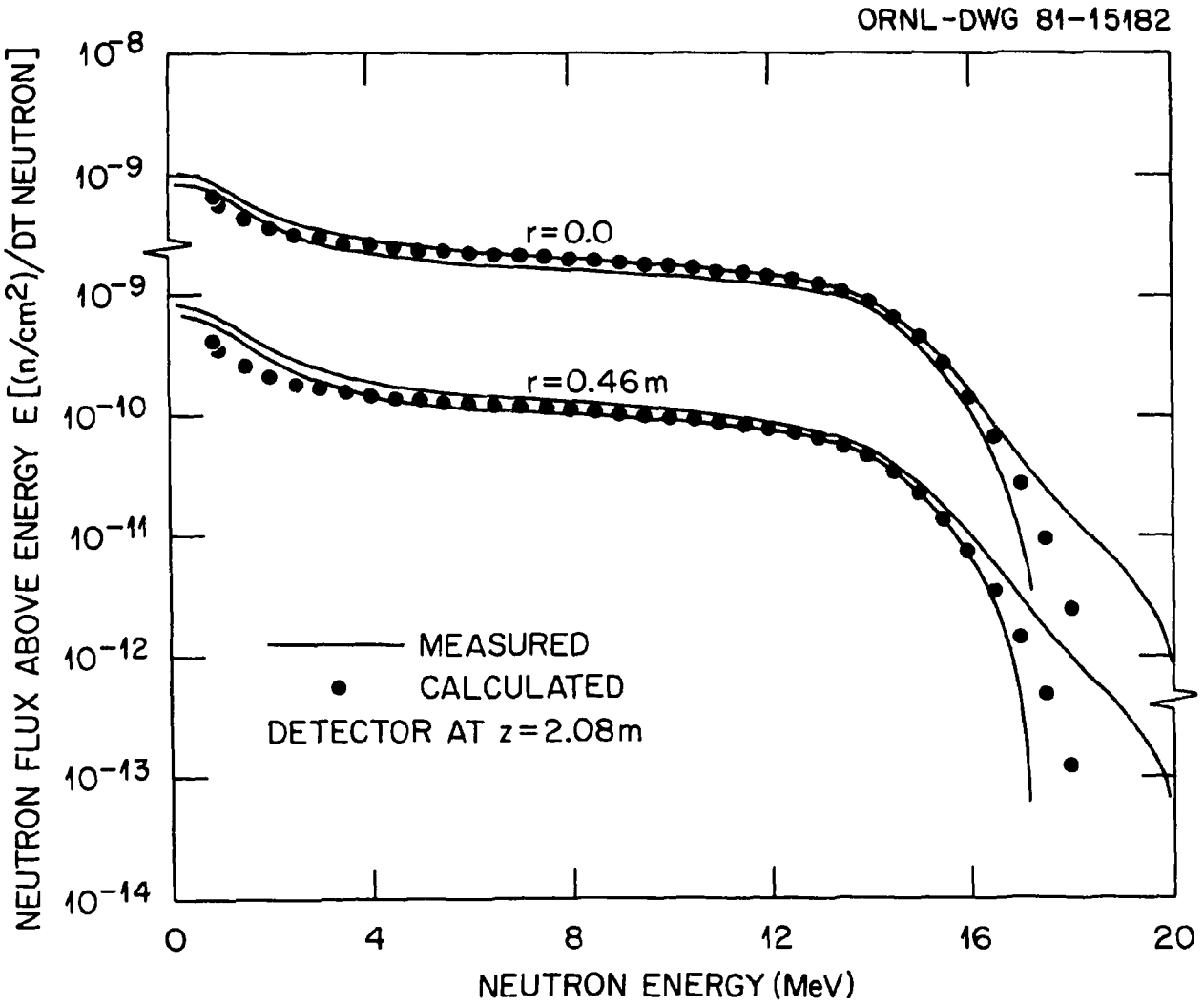

Fig. 14. Neutron flux above energy E vs. neutron energy for the 0.80-m-thick SS-304-BP assembly for the detector at z = 2.08 m, r = 0.0 and r = 0.46 m. (Note break in the ordinate)

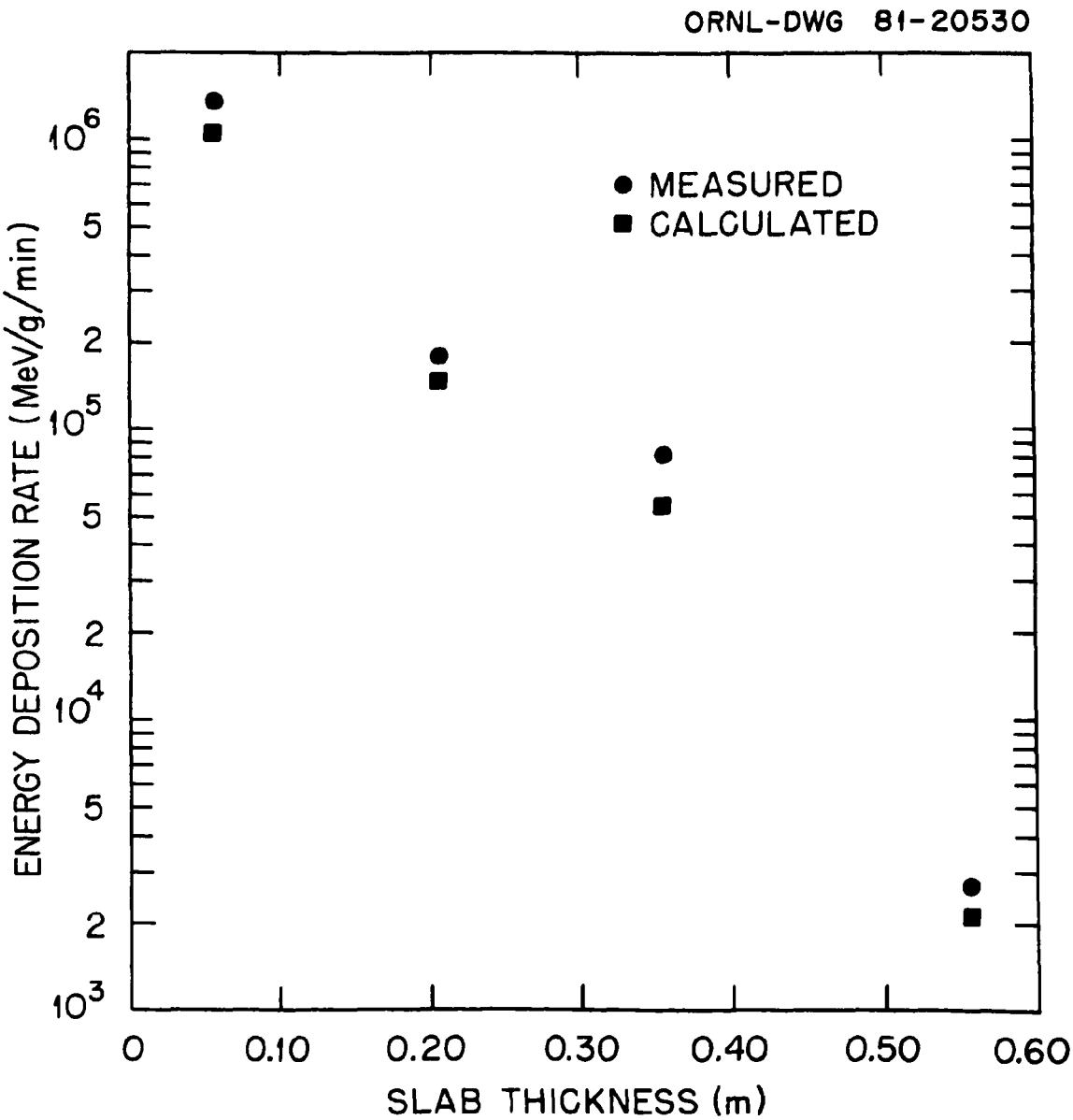

Fig. 15. Gamma-ray energy deposition rate vs. slab thickness in the 0.80-m-thick SS-304-BP assembly.

References

1. R. T. Santoro, R. G. Alsmiller, Jr., J. M. Barnes, G. T. Chapman, "Calculation of Neutron and Gamma-Ray Energy Spectra in Fusion Reactor Shield Design: Comparison with Experiment," Nucl. Sci. Eng. 78, 259 (1981).
2. R. T. Santoro, R. G. Alsmiller, Jr., J. M. Barnes, G. T. Chapman, J. S. Tang, "Calculated Neutron and Gamma-Ray Energy Spectra from 14-MeV Neutrons Streaming Through an Iron Duct: Comparison with Experiment," ORNL/TM-7878, Oak Ridge National Laboratory (1981) submitted for Journal publication.
3. R. T. Santoro, R. G. Alsmiller, Jr., J. M. Barnes, E. M. Oblow, "Calculational Procedures for the Analysis of Integral Experiments for Fusion Reactor Design: Attenuation Experiments," ORNL-5777, Oak Ridge National Laboratory (1981).
4. G. T. Chapman, G. L. Morgan, and J. W. McConnell, "The ORNL Integral Experiments to Provide Data for Evaluating the MFE Shielding Concepts. Part I: Attenuation Measurements," ORNL/TM-7356, Oak Ridge National Laboratory (to be published).
5. W. R. Burrus and V. V. Verbinski, Nucl. Instrum. Methods 67, 181 (1979).
6. R. A. Lillie, R. G. Alsmiller, Jr. and J. T. Mihalczo, "Design Calculations for a 14-MeV Neutron Collimator," Nucl. Technol. 43, 373 (1979).

7. W. A. Rhoades and F. R. Mynatt, "The DOT III Two-Dimensional Discrete Ordinates Transport Code," ORNL/TM-4280, Oak Ridge National Laboratory (1979).

8. "FALSTF, Informal Notes," CCC-351, Radiation Shielding Information Center, Oak Ridge National Laboratory (1974).

9. R. W. Roussin, C. R. Weisbin, J. E. White, N. M. Greene, R. Q. Wright, J. B. Wright, "The CTR Processed Multigroup Cross Section Library for Neutronics Studies," ORNL/RSIC-37, Radiation Shielding Information Center, Oak Ridge National Laboratory (1975); also available as DLC-41.

10. W. W. Engle, Jr., "A User's Manual for ANISN, A One-Dimensional Discrete Ordinates Code with Anisotropic Scattering," K-1693, Oak Ridge National Laboratory (1967).

11. "BUGLE, Coupled 45-Neutron, 16-Gamma-Ray, P_3, Cross Sections for Studies by the ANS 6.1.2 Shielding Standards Working Group on Multigroup Cross Sections," DLC-47 Radiation Shielding Information Center, Oak Ridge National Laboratory (1977).

12. R. E. Maerker, "Analysis of the TSF Experiments on Radiation Heating in a Stainless Steel Sodium CRBR Radial Shield Mock-Up Using a 32-Inch Diameter Collimated Beam Source," ORNL/TM-5992, Oak Ridge National Laboratory (1977).